Separation and Purification Technology 259 (2021) 118094

Contents lists available at ScienceDirect

Separation and Purification Technology

journal homepage: www.elsevier.com/locate/seppur

# Design of nanofiltration cascades for fructooligosaccharides using the McCabe-Thiele approach

Zulhaj Rizki [a,*], Anja E.M. Janssen [a], Albert van der Padt [a,b], Remko M. Boom [a]

[a] Wageningen University, Food Process Engineering Group, PO Box 17, 6700 AA Wageningen, the Netherlands
[b] FrieslandCampina, Stationsplein 4, Amersfoort 3818 LE, the Netherlands

ARTICLE INFO

*Keywords:*
Membrane cascades
Nanofiltration
Oligosaccharides
Design method
McCabe-Thiele method

ABSTRACT

We developed a design method for an inhomogeneous membrane cascade by adopting the McCabe-Thiele method, which is long established for designing distillation columns. The stage cut value is an independent design parameter in the design procedure and thus has to be set. Within each section, the operating conditions were uniform, but both sections could be operated differently using various combinations of membranes, transmembrane pressure, temperature and stage cut. The procedure was applied to cascaded nanofiltration for the fractionation of a mixture of fructooligosaccharides of varying molecular weight. The stage and area requirements were strongly dependent on the initial design parameter, the overall stage cut. The total area was related to the overall system cut. However, the overall system cut was dependent on the stage cuts for both sections (top and bottom). The top stage cut could be chosen, whereas the bottom stage cut needed to be calculated iteratively to match the top design at the intersection.

## 1. Introduction

Nanofiltration is a common process to purify fructooligosaccharides (FOS) from a mixture, which appears in natural sources such as chicory as a mixture of oligosaccharides with various degrees of polymerization (DP). Both nutritional and functional properties of FOS are dependent on the DP. FOS with high DP have higher prebiotic activity, have a blander taste and higher viscosity [1–4]. These properties are less pronounced at lower DP, and the opposite properties are found in their monosaccharides: fructose and glucose. However, these monosaccharides also appear in the mixture so they need to be removed. Considering the molecular weights of both the mono- and disaccharides and the only somewhat larger oligosaccharide molecules, nanofiltration is deemed a suitable process to separate them [5–7].

A single step FOS nanofiltration will not give a good resolution related to the similar molecular weights between the FOS components. Improving the separation process can be done by either improving the membrane selectivity [8,9] or by a different system design. Without using an improved membrane, the separation performance can be enhanced using a multi-stage process [10–12]. Recycling the non-product streams (counter-current) to the previous stage makes the separation more efficient due to loss reduction [10,11,13,14]. Such a design is known as a membrane cascade.

The ideal membrane cascade concept assumes the same separation in each stage and imposes a "no-mixing" condition in the system [15,16]. This implies that all streams entering the mixing points anywhere in the cascade should have similar concentrations. This condition is not easily achievable in practice. Lifting this constraint gives us more freedom to have different conditions and settings at each stage (inhomogeneous cascades) [17–19].

Recent studies on the use of inhomogeneous cascades for FOS separation report an enhanced separation performance with only a limited number of stages [17,20]. This was achieved by modifying the stream configurations and operating conditions at each stage using a three-stage cascade. However, even at this newfound optimum, a three-stage cascade has its limits [21]. Addition of stages does improve the product purity [19], but there is still no systematic procedure to determine the required number of stages to achieve a certain purity target.

The McCabe-Thiele method to design a counter-current system was developed in 1925 for distillation [22]. This is a graphical procedure to design binary distillation systems. In this method, an equilibrium curve that represents the vapor-liquid equilibrium of the mixture is plotted, representing the composition after 1 stage of separation. Two operating lines are drawn between the equilibrium curve and the parity curve ($x = y$), which are based on the mass balances for the top and the bottom

* Corresponding author.
*E-mail address:* zulhaj.zulhajrizki@wur.nl (Z. Rizki).

https://doi.org/10.1016/j.seppur.2020.118094
Received 7 August 2020; Received in revised form 8 October 2020; Accepted 17 November 2020
Available online 21 November 2020
1383-5866/© 2020 The Authors. Published by Elsevier B.V. This is an open access article under the CC BY license (http://creativecommons.org/licenses/by/4.0/).

**Nomenclature**

| | |
|---|---|
| $A$ | area [$m^2$] |
| $c$ | solute concentration [g $L^{-1}$] |
| $F$ | flow rate [kg $h^{-1}$] |
| $Jv$ | volumetric flux [$m^3$ $m^{-2}$ $s^{-1}$] |
| $R_o$ | observed rejection [dimensionless] |
| $T$ | process temperature [K] |
| TMP | trans-membrane pressure [Pa] |
| $VR$ | section volume reduction [dimensionless] |
| $x$ | mass fraction [dimensionless] |

*Greek letters*

| | |
|---|---|
| $\alpha$ | separation factor [dimensionless] |
| $\theta$ | stage cut [dimensionless] |

*Subscripts*

| | |
|---|---|
| $A, B$ | component |
| top, bottom | section indication |
| $m$ | stage number at the bottom section |
| $n$ | stage number at the top section |
| $p$ | permeate side |
| $r$ | retentate side |

section. The number of required stages is then represented by a stair-like pattern that goes back and forth toward the equilibrium curve and the operating lines.

The similarities between distillation and a counter-current recycled membrane cascade system are generally acknowledged [23–25]. The counter-current recycling streams in the cascade resemble the counter-current flows in the distillation column. Instead of the vapor and liquid flows, the streams in the cascade are presented by the permeate and retentate streams among stages. The equilibrium between the liquid and the vapor in every stage of a distillation column is analogous to the partitioning between permeate and retentate in every stage of the cascade.

Despite the similarities between distillation and the membrane cascade, only a few studies have been published about the McCabe-Thiele method for designing membrane cascades. Siew et al. [14,26] reported the adaptation of McCabe-Thiele to design an organic solvent nanofiltration cascade. They constructed the McCabe-Thiele curves based on the concentration of the solute that becomes more concentrated in every stage. However, this adaptation is not suitable for a binary mixture, which should give fractions with some degree of purity. Vanneste et al. [27] used the McCabe-Thiele method to evaluate the economic aspects of the membrane cascade design and compared it with simulated moving bed chromatography. Recently, Lejeune et al. [24,28] reported an adaptation of the McCabe-Thiele approach for a binary mixture in an ideal organic solvent nanofiltration cascade. However, the scope of that study was limited to an ideal design in which no mixing was allowed in the system. In this article, we extend the McCabe-Thiele approach to design a non-ideal, inhomogeneous cascade for FOS purification. This allows different operating conditions among the stages and yields the required membrane surface areas and pressure.

## 2. Development of the graphical method

The McCabe-Thiele graphical layout consists of 2 major components: the partitioning curve and the operating lines. Both the curve and the lines are plotted in an $x$-$y$ diagram. The mass fraction of 1 component in the permeate ($x_p$) is on the vertical axis and the mass fraction in the retentate ($x_r$) is on the horizontal axis. The permeate streams are analogous to the vapor up-flow and the retentate is analogous to the liquid down-flow in the distillation column. The mixture is considered as a binary mixture, neglecting the water as solvent in this case, with the most retained component used as the base concentration.

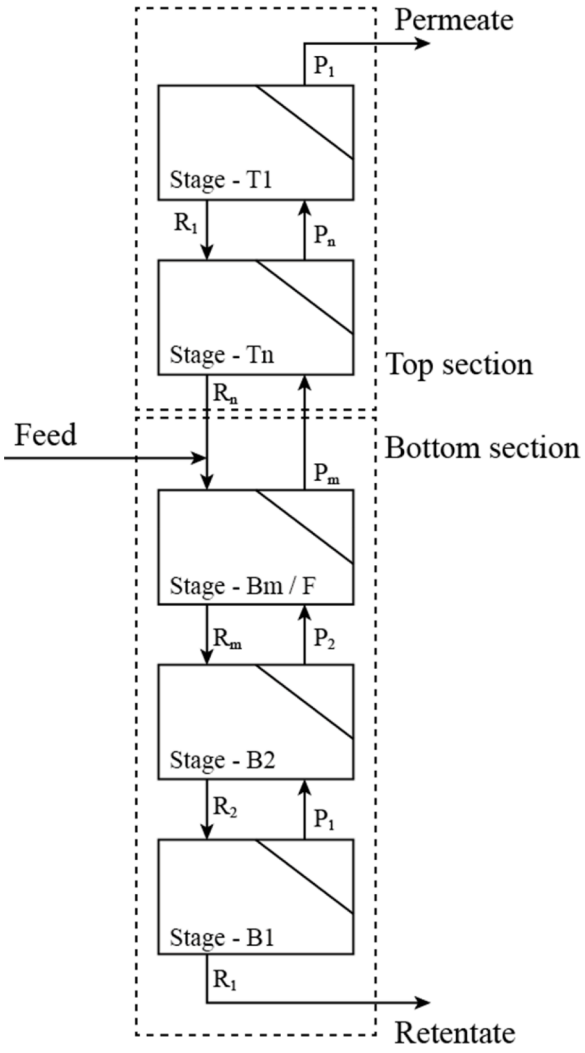


**Fig. 1.** Graphical representation of a membrane cascade design with $n$ stage at the top section and $m$ stage at the bottom section.

$$x_B = \frac{c_B}{c_B + c_A} \tag{1}$$

The feed enters the cascade with a known mass fraction, $x_{feed}$. The desired products exits at the top and bottom section with the desired mass fraction, $x_{p,top}$ and $x_{r,bottom}$.

### 2.1. Partitioning curve

The partitioning curve gives the mass fraction of the permeate that is obtained for a specific retentate. Both fractions are related in a parameter called the separation factor, $\alpha$, as shown in Eq. (2) [24].

$$\alpha = \frac{x_p/1 - x_p}{x_r/1 - x_r} \tag{2}$$

Most membranes are characterized by their rejection coefficient (Eq. (3)), which relates the concentration at both the permeate and retentate.

$$R_{o,c} = 1 - \frac{c_{p,c}}{c_{r,c}} \tag{3}$$

Here, we use the observed rejection coefficient; its value is observed under practical conditions and deviates from the real rejection due to

concentration polarization phenomena. To construct the partitioning curve using a known rejection value, a relationship between them needs to be defined. Lejeune et al.[24] expressed the separation factor, $\alpha$, independently of the mass fraction, with a design parameter. We define the fraction of the feed that becomes the permeate as the stage cut, $\theta$ (Eq. (4)), which is an input design parameter to be set. Rewriting the equations derived in the work of Lejeune et al., the separation factor, $\alpha$, gives Eq. (5). In this equation, subscripts $A$ and $B$ represent the component, $k$, in a binary mixture, with $B$ as the most retained component.

$$\theta = \frac{F_p}{F_f} \tag{4}$$

$$\alpha = \frac{\left(c_{f,A}/c_{p,A}\right) - \theta}{\left(c_{f,B}/c_{p,B}\right) - \theta} \tag{5}$$

The concentration ratio between feed and retentate was derived to be dependent on the stage cut and the rejection (Eq. (6)), with $k$ equal to either $A$ or $B$.

$$\frac{c_{p,k}}{c_{f,k}} = \frac{1}{\theta}\left[1 - (1-\theta)^{1-R_{o,k}}\right] \tag{6}$$

Hence, the partitioning curve depends on 1 independent design parameter, the stage cut $\theta$, and 1 system parameter, the rejection coefficient, $R_{o,c}$. The rejection coefficient of a membrane can be characterized and predicted at given operating conditions, e.g., trans-membrane pressure (TMP) and temperature [29]. With this value we can plot the partitioning curve using Eq. (2).

### 2.2. Operating lines

The partitioning curve represents the composition of the permeate streams at every stage, and the operating lines represent the component fractions of the incoming streams, given by a mass balance with the incoming streams coming from the previous stage and the recycle from the consecutive stage (Fig. 1). Therefore, the operating lines relate the component fractions at one particular stage to the adjacent stage. Fig. 1 shows a graphical representation of a membrane cascade system.

The cascade consists of 2 sections: the top and the bottom section. In some reports [14,18,19], the feed stage is considered as a third section. To simplify the design, the feed stage can be considered to be part of the bottom section, as was proposed by Avgidou et al. [30]. In this case, the feed stage follows the design conditions of the bottom section. Fig. 1 shows the streams in stage $n$ at the top section and stage $m$ in the bottom section. The stage number for both sections starts from both products and ends at the mid-point where the feed stream enters.

Each stage is operated with its own stage cut. However, in this approach, the stage cut values for the whole section are kept the same. This leaves only 2 stage cut values: the stage cut of the top section, $\theta_{\text{top}}$, and the stage cut of the bottom section, $\theta_{\text{bottom}}$.

The equations for the operating lines can be derived via mass balances throughout the cascade, which can be evaluated separately for both the top and bottom sections. Detailed derivation for the operating lines can be found in the work of Hwang and Kammermeyer [31] and Avgidou et al. [30]. In this section, we summarize the equations that are used for the design.

Derived from the total and component mass balances, the operating line in the top section can be expressed by Eq. (7) [30].

$$x_{p,n+1} = \frac{\sum_{i=1}^{n}\left(\prod_{j=i}^{n}\gamma_{\text{top,j}}\right)}{1+\sum_{i=1}^{n}\left(\prod_{j=i}^{n}\gamma_{\text{top,j}}\right)}x_{r,n} + \frac{1}{1+\sum_{i=1}^{n}\left(\prod_{j=i}^{n}\gamma_{\text{top,j}}\right)}x_{p,\text{top}} \tag{7}$$

with

$$\gamma_{\text{top}} = \frac{1-\theta_{\text{top}}}{\theta_{\text{top}}} \quad for\ all\ stage\ n \tag{8}$$

In the ideal cascade design evaluated by Lejeune et al. [24], a non-mixing condition must be obeyed. To achieve this, every stage must be operated using different stage cut values. On the other hand, a constant stage cut within stages in the top section can be achieved by allowing a mixing condition for streams that enter a particular stage (non-ideal design). Avgidou et al. [30], also evaluated the non-ideal cascade with the restriction of a constant stage cut within the section. In this case, Eq. (7) can be simplified into Eq. (9).

$$x_{p,n+1} = \frac{\gamma_{\text{top}}\left(\frac{\gamma_{\text{top}}{}^{n}-1}{\gamma_{\text{top}}-1}\right)}{1+\gamma_{\text{top}}\left(\frac{\gamma_{\text{top}}{}^{n}-1}{\gamma_{\text{top}}-1}\right)}x_{r,n} + \frac{1}{1+\gamma_{\text{top}}\left(\frac{\gamma_{\text{top}}{}^{n}-1}{\gamma_{\text{top}}-1}\right)}x_{p,\text{top}} \tag{9}$$

The operating line that is expressed by either Eq. (7) or Eq. (9) represents a linear equation that gives different slopes for each stage (each value of $n$). Nevertheless, all these lines share a pivot point, $x_{p,\text{top}}$, which is the target concentration. This indicates that the operating lines need to be evaluated for every stage despite the constant stage cut.

Similar to the top operating line, the bottom operating line can be derived from the mass balances and is expressed in Eq. (10) and simplified into Eq. (11) for a non-ideal cascade with constant stage cut. These equations also show a dynamic linear equation that pivots the target point, $x_{r,\text{bottom}}$.

$$x_{p,m} = \frac{1+\sum_{i=1}^{m}\left(\prod_{j=i}^{m}\frac{1}{\gamma_{\text{bottom,j}}}\right)}{\sum_{i=1}^{m}\left(\prod_{j=i}^{m}\frac{1}{\gamma_{\text{bottom,j}}}\right)}x_{r,m+1} + \frac{1}{\sum_{i=1}^{m}\left(\prod_{j=i}^{m}\frac{1}{\gamma_{\text{bottom,j}}}\right)}x_{r,\text{bottom}} \tag{10}$$

$$x_{p,m} = \frac{\frac{1}{\gamma_{\text{bottom}}}\left(\frac{\frac{1}{\gamma_{\text{bottom}}}{}^{m}-1}{\frac{1}{\gamma_{\text{bottom}}}-1}\right)+1}{\frac{1}{\gamma_{\text{bottom}}}\left(\frac{\frac{1}{\gamma_{\text{bottom}}}{}^{m}-1}{\frac{1}{\gamma_{\text{bottom}}}-1}\right)}x_{r,m+1} - \frac{1}{\frac{1}{\gamma_{\text{bottom}}}\left(\frac{\frac{1}{\gamma_{\text{bottom}}}{}^{m}-1}{\frac{1}{\gamma_{\text{bottom}}}-1}\right)}x_{r,\text{bottom}} \tag{11}$$

with

$$\gamma_{\text{bottom}} = \frac{1-\theta_{\text{bottom}}}{\theta_{\text{bottom}}} \quad for\ all\ stage\ m \tag{12}$$

The dynamic characteristic of both top and bottom operating lines for membrane cascades distinguishes this method from the original McCabe-Thiele method for distillation. In distillation, a single line exists for every section. All stages are built up using these lines. In addition, the graphical method for membrane cascades does not use a q-line that represents the state of the feed stream. Instead, the stage cut at both sections should be chosen in such a way that the concentrations at the end of both sections match.

In the distillation column, an equimolar exchange between the liquid and vapor exists in each stage. Therefore, the inter-stage flows can be maintained constant. This condition can be represented by a single operating line for each section. To ensure that this condition occurs in every stage, the distillation column requires a reflux from the top stage and a reboiler at the bottom. These conditions do not exist in the membrane cascade, which gradually creates flow along the cascade stages. This condition explains the dynamic behavior of the operating lines as derived in the work of Avgidou et al. [30].

### 2.3. Overall system cut and total area

Referring to the work of Avgidou et al. [30], the ratio between the permeate stream coming to the top section and the outlet permeate stream can be expressed with Eq. (13). To simplify the calculations, this parameter can be defined as the volume reduction at the top section,

**Table 1**
Feed condition for designing an inhomogeneous nanofiltration cascade for FOS purification.

| Parameter | Notation | Unit | Values[a] |
|---|---|---|---|
| Sugar concentration | $c_{feed,sugar}$ | g/L | 9.04 ± 0.16 |
| FOS concentration | $c_{feed,FOS}$ | g/L | 31.49 ± 0.47 |
| Feed mass fraction (FOS) | $x_{feed}$ | | 0.78 ± 0.01 |
| Feed flow rate (design) | $F_{feed}$ | kg/h | 50 |

[a] Uncertainties were calculated based on the 95% confidence interval.

$VR_{top}$. The expression for the retentate leaving this section can then be expressed in Eq. (14).

$$VR_{top} = \frac{F_{p,n+1}}{F_{p,top}} = \left(\frac{1}{\theta_{top}} - 1\right)\left[\frac{\left(\frac{1}{\theta_{top}} - 1\right)^{n} - 1}{\frac{1}{\theta_{top}} - 2}\right] + 1 \tag{13}$$

$$F_{r,n} = \left(VR_{top} - 1\right)F_{p,top} \tag{14}$$

Similarly, the ratio of the retentate stream coming to the bottom section and the outlet retentate can be defined as the volume reduction at the bottom section, $VR_{bottom}$, and is expressed in Eq. (15).

$$VR_{bottom} = \frac{F_{r,m+1}}{F_{r,bottom}} = \left(\frac{\theta_{bottom}}{1 - \theta_{bottom}}\right)\left[\frac{\left(\frac{\theta_{bottom}}{1-\theta_{bottom}}\right)^{m} - 1}{\left(\frac{\theta_{bottom}}{1-\theta_{bottom}}\right) - 1}\right] + 1 \tag{15}$$

At the upper stage of the bottom section, where the feed stream enters, the retentate coming from the top section is mixed with the feed stream. Therefore, the stream coming to the bottom section can be expressed with Eq. (16).

$$F_{r,m+1} = F_{r,n} + F_{feed} \tag{16}$$

By rearranging Eqs. (14), (15) and (16), we can calculate the overall system cut, which is defined as the ratio of the permeate stream coming out of the top section to the feed stream (Eq. (17)).

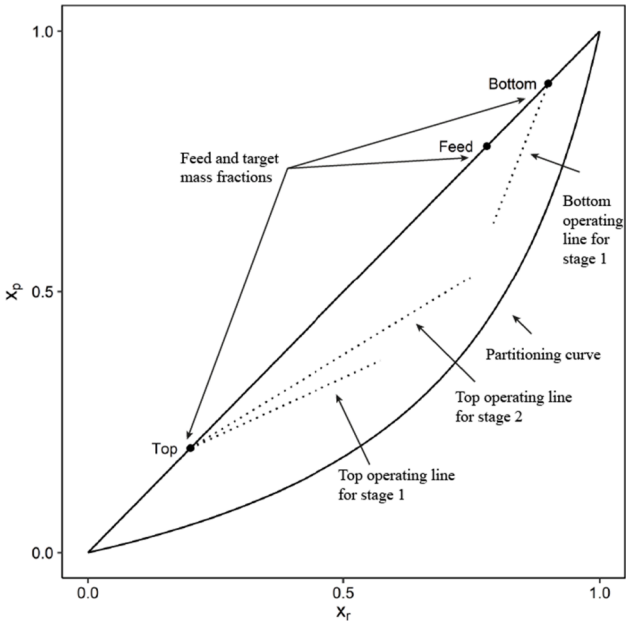


**Fig. 2.** Illustration of partitioning curves, operating lines and feed and target points in the McCabe-Thiele diagram.

$$\theta_{all} = \frac{F_{p,top}}{F_{feed}} = \frac{VR_{bottom} - 1}{VR_{top} + VR_{bottom} - 1} \tag{17}$$

With a given feed stream as the basis of the design and the chosen stage cut as the design parameter, we can calculate all streams in the cascade. These include the 2 outlet streams from both the top and bottom sections and the inter-stage stream coming from and to 2 adjacent stages. With known permeate flow in each stage, we can calculate the required area, $A_{stage}$, by dividing it with its standard flux, $J_v$. The standard flux for each membrane is normally characterized under certain operating conditions (TMP and temperature). Therefore, the total area required for a design can then be formulated as the sum of the total area in the top section (with $n$ stage) and the bottom section (with $m$ stage) (Eq. (19)).

$$A_{stage} = \frac{F_{p,stage}}{J_v(\mathrm{TMP}, T)} \tag{18}$$

$$A_{total} = \sum_{i=1}^{n} A_i + \sum_{j=1}^{m} A_j \tag{19}$$

## 3. Methods and calculations

### 3.1. Filtration setup

The McCabe-Thiele method adopted here was applied to the design of an inhomogeneous nanofiltration cascade to purify a FOS mixture with a molecular weight distribution. The feed stream was based on 5% dilution of Frutalose L85. The experiments to characterize the membranes were performed in the previous research [29]. In this paper, the experimental results were reanalyzed for design purpose. The FOS mixture was considered as a binary mixture of sugars and FOS. The sugars comprise mono- and disaccharides and FOS comprises the oligosaccharides with DP of 3 and higher.

The feed entered the cascade with a flow rate, $F_{feed}$, of 50 kg/h and mass fraction, $x_{feed}$, of 0.78. Details on the feed conditions are summarized in Table 1.

The design considers 3 different types of nanofiltration membranes, namely GE with molecular weight cutoff (MWCO) of 1 kDa, GH with MWCO of 2.5 kDa and GK membrane with MWCO of 3.5 kDa. Although the module size was not fixed in this design, the membrane properties are assumed to be similar. The 3 membranes have been characterized in the previous study [29] between TMP 4 and 16 bar and operating temperature between 25 °C and 45 °C. The rejection and flux of all 3 membranes within the scope can therefore be predicted using a model.

### 3.2. Design method

We adopted a non-ideal cascade with a constant operating parameter for each section. The design and operating parameters, which included the membrane, TMP, temperature and stage cut, were chosen independently for each section. The design process started with the top section and continued with the bottom one.

In this study, a standard target (design A) was chosen arbitrarily as 0.2 at the top, $x_{p,top}$, and 0.9 at the bottom, $x_{r,bottom}$. These values are equivalent with 90% purity of FOS at the bottom and 80% purity of sugars at the top. We also discuss other target concentrations to demonstrate the effect of changing these targets in the design. The feed concentration, $x_{feed}$, and both targets can be indicated on the diagonal line in the McCabe-Thiele plot.

The partitioning curve was plotted using Eqs. (2)–(6). For this, we need the rejection coefficients for both sugars and FOS as well as the stage cut. The rejection coefficient was calculated via a model [29]. This model predicts the rejection of FOS molecule with given feed composition, at a selected membrane type, TMP and temperature. The rejection was predicted for each component in the FOS mixture regarding to its

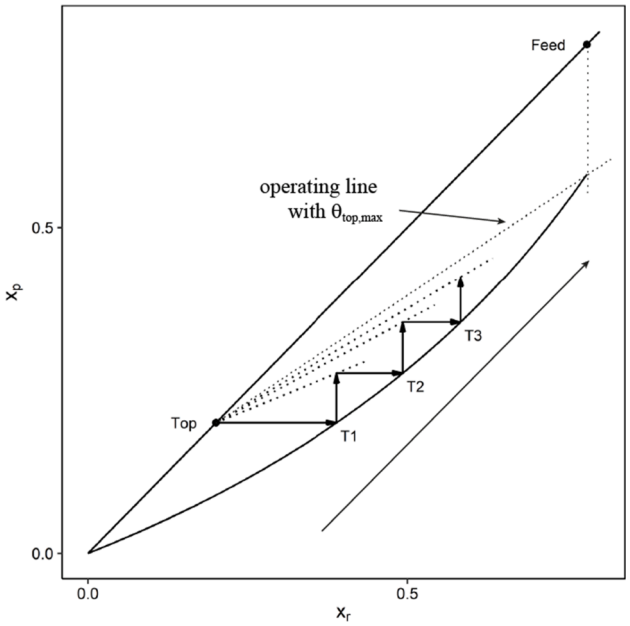


**Fig. 3.** Illustration of stage build up in the top section in the McCabe-Thiele diagram for the membrane cascade.

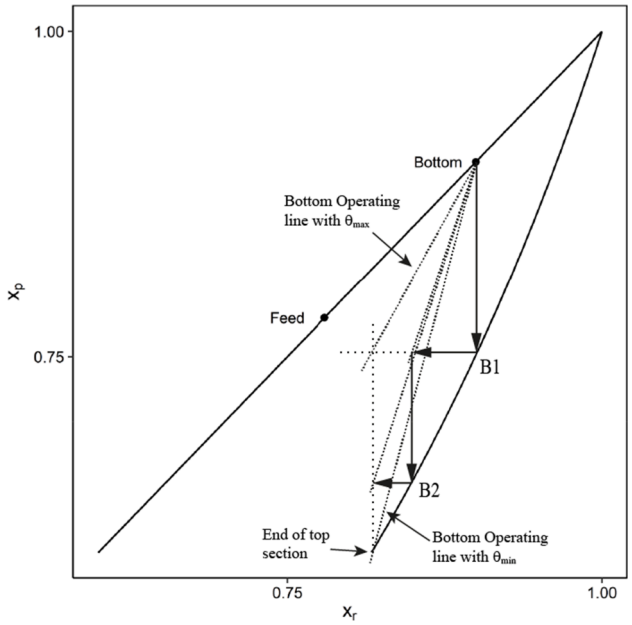


**Fig. 4.** Illustration of stage build up in the bottom section in the McCabe-Thiele diagram for the membrane cascade.

degree of polymerization. For design purpose in this paper, those rejection values were recalculated by clustering the carbohydrate components into sugars and FOS. The stage cut for the top section, $\theta_{top}$, can be chosen arbitrarily as long as it does not exceed its maximum value. A larger stage cut implies more stages; a small stage cut implies larger volumes between each stage and therefore more membrane area. At the maximum value of the stage cut, the required number of stages at the top section becomes infinite. In the McCabe-Thiele plot, this is illustrated by the operating line that passes through the partitioning curve with the retentate concentration similar to the feed. At this point, the permeate concentration can be calculated using Eq. (2). The maximum stage cut theoretically gives an infinite number of stages, thus the stage number, $n$, in Eq. (8) should be infinite. Computationally, this number can be approached with an arbitrarily large number (e.g. 50). With known $x_r$, $x_p$ and $n$, Eq. (8) becomes an equation with just 1 variable, $\theta_{top}$. Solving this equation, which is a basic root-finding algorithm, will give the value of maximum $\theta_{top}$.

Using a stage cut larger than the maximum will create a design that cannot meet the bottom section. A stage cut of 0 means a minimum number of stages, but an infinitely large membrane area, because all retentates and permeates are fed back into the system (comparable to 100% reflux in distillation). Thus, we need to make a reasonable choice in between these 2 extremes. We here select a $\theta_{top}$ of 75% from its maximum.

With this value, we could plot the operating lines at the top section using Eq. (8). The partitioning curve, the feed and target points and the operating lines are illustrated in Fig. 2.

Once the partitioning curve and the operating lines are constructed, we can start building the stages. The concentrations of the permeate streams of any stage are represented by the partitioning curve. The inlet concentration is related to the outlet concentration via the operating lines. Therefore, the stages can be built up with alternating horizontal and vertical lines going from and to both the partitioning curve and the operating lines. The target at the top section comes out of the first stage at the permeate side concentration of $x_{p,top}$. To draw the first stage in the McCabe-Thiele diagram, we draw a horizontal line from the top target point toward the partitioning curve. A line is then drawn vertically toward the operating line. This procedure is repeated until the end of the top section. The end of the top section is indicated by a retentate concentration, $x_{r,n}$, which exceeds the feed concentration, $x_{feed}$. Building up the stages in the top stages is illustrated in Fig. 3.

Designing the bottom section is done similarly. From the bottom target, we draw the vertical line to the partitioning curve and then draw a line vertically to the operating curve. This procedure was repeated until it met the end of the top section.

A challenge in designing the bottom section is that the stage cut must be chosen such that the end point of the bottom section exactly meets the end point of the top section. This meeting point could be after any number of stages. As a consequence, an iterative procedure is required in designing the bottom section by changing the stage cut value until the end point matches the top section. To aid the calculation, the iteration was done between 2 extreme stage cuts: the minimum and maximum stage cut. The minimum stage cut would cause an infinite number of stages in the design. This condition was illustrated with the operating lines that intersect the end of top section. The maximum stage cut was the stage cut at which the operating line caused only 1 stage at the bottom. The bottom stage must have at least 1 stage: the feed stage. The illustration of building up the bottom section is presented in Fig. 4.

After designing the bottom section, we calculate the overall system cut, $\theta_{all}$. Using this parameter, we can then calculate both outlet flows and the inter-stage flows. This then lets us calculate the area for every stage and for the total system. This conclude the design procedure. A summary of the design procedure for a membrane cascade system using the McCabe-Thiele method is shown in Fig. 5.

Here, we demonstrate the use of the design procedure by evaluating 11 designs with differing operating conditions and targets. Design A was chosen as reference, which uses only GH membranes operated at 16 bar and 45 °C. This design was constructed to reach a bottom target, $x_{r,bottom}$, of 0.9 and a top target, $x_{p,top}$, of 0.2. Designs B to E use a similar configuration as design A to attain different targets. Design F uses a similar configuration as design A, but using GE membranes; design G uses GK membranes. These 7 designs are all based on a uniform design in which the type of membrane and operating conditions are the same at all stages in the cascade. In addition, we also evaluated hybrid, inhomogeneous designs (H–K) with various combinations of membrane, TMP and temperature at the top and bottom sections. Details of all 11 designs are shown in Table 2.

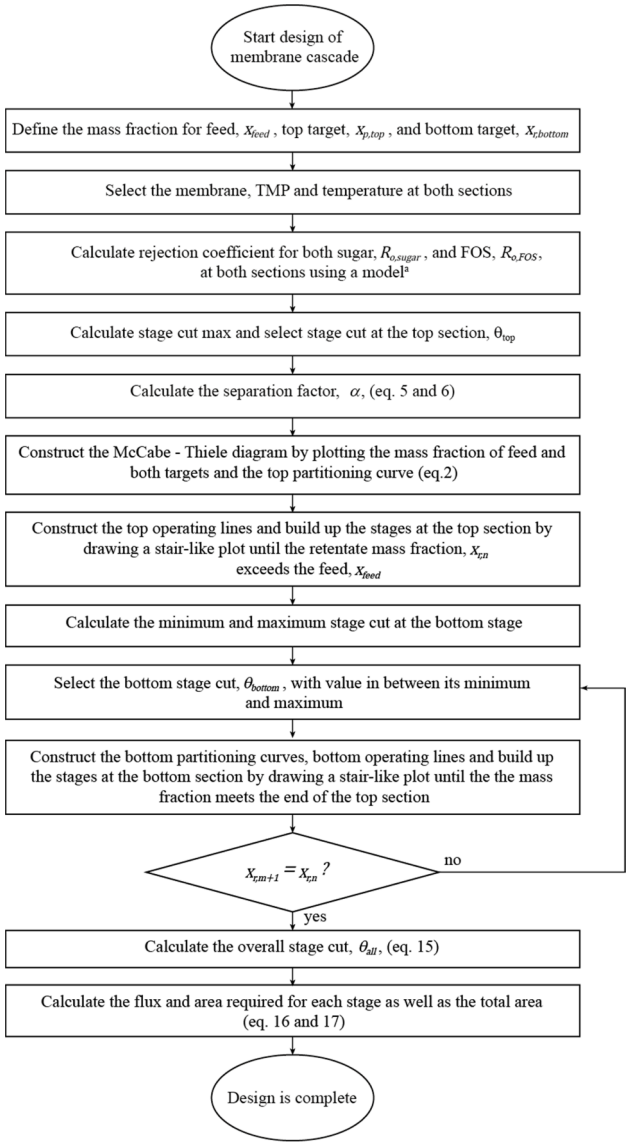


**Fig. 5.** Flowchart of the design procedure for the membrane cascade using the McCabe-Thiele method. [a]The rejections were predicted using a model developed in a previous work [29].

## 4. Results and discussion

### 4.1. Effect of various operating conditions

#### 4.1.1. Partitioning curves for different membranes, TMPs and temperatures

The partitioning curves were drawn for the 3 membranes considered in this study. The membranes vary in their MWCO, which affects their separation factor, $\alpha$. A higher separation factor indicates better separation, implying less stages are required for a separation. In the McCabe-Thiele diagram, this is indicated by a partitioning curve that is situated farther away from the diagonal parity line. The minimum stage requirement is a theoretical number of stages needed in the cascade to achieve the separation target. This represents a system in which the product streams fully re-enter the system as reflux, and an infinite membrane area is needed. This was obtained by building up the stages as explained in Section 3.2. Instead of the operating lines, the diagonal line was used. The diagonal line is theoretically the operating line at stage cut 0. That means, all streams goes to the retentate and no top product is acquired; this extreme condition does not exist in practice, of course.

Fig. 6 shows the partitioning curves and illustrates the minimum stage requirement for the 3 membranes. We can see that the GE membrane has the widest partitioning curve and the GK membrane has the narrowest. The partitioning curve for both GE and GH were close to each other and both membranes require the same minimum number of stages. However, the GE membrane has a lower flux than the GH membrane, which results in a larger membrane surface area requirement.

The curvature of the partitioning curve is dependent on the operating conditions, because these affect the rejection coefficient. A higher rejection can be achieved at a higher TMP and a lower temperature. However, we found the opposite effect of the TMP in the partitioning curve. In fact, a wider curve was found at lower TMP (Fig. 7), indicating better separation at lower TMP. The temperature effect in the partitioning curve was as expected, giving a wider curve at lower temperatures.

According to Eqs. (2)–(6), the partitioning curve is not solely dependent on the rejection coefficient. Instead, it is dependent on the separation factor, $\alpha$, between 2 components of interest. The temperature effect in the rejection is linear [29], therefore we can expect the same effect for the separation factor. The effect of TMP in the rejection is more complex. The TMP affects the convective transport in the nanofiltration system, which is not linear. The effect is more prominent for smaller molecules [29,32]. As a result, the separation between the 2 grouped components was better at low TMP. Fig. 8 shows contour plots for the separation factor, $\alpha$, as a function of TMP and operating temperature, for all 3 membranes. A combination of a low TMP and a low temperature gives a low $\alpha$, and thus a wider partitioning curve. Referring to Fig. 8, we can select a combination of TMP, temperature and membrane that gives a certain value of $\alpha$; any system that is on the same contour line would give the same partitioning curve. This figure also shows that GE and GH membranes have an overlapping operating window with similar separation.

#### 4.1.2. Partitioning curves and operating lines with various stage cuts

In addition to the selection of the type of membrane and the operating conditions, the value of the stage cut affects both the partitioning curve and the operating lines. However, its effect on the operating lines is stronger (Fig. 9). The partitioning curve relates the concentrations in the permeate and retentate for each stage, calculated from the real rejection coefficient, which is independent of the flow rates. The partitioning curve is constructed with the observed rejection, which deviates

**Table 2**
Operating conditions for the 11 designs evaluated in this study.

| Parameter | | Unit | Design | | | | | | | | | | |
|---|---|---|---|---|---|---|---|---|---|---|---|---|---|
| | | | A | B | C | D | E | F | G | H | I | J | K |
| Target (mass fraction) | Top | | 0.2 | 0.1 | 0.3 | 0.2 | 0.2 | 0.2 | 0.2 | 0.2 | 0.2 | 0.2 | 0.2 |
| | Bottom | | 0.9 | 0.9 | 0.9 | 0.85 | 0.95 | 0.9 | 0.9 | 0.9 | 0.9 | 0.9 | 0.9 |
| Operating condition (top) | Membrane | | GH | GH | GH | GH | GH | GE | GK | GH | GE | GH | GE |
| | TMP | bar | 16 | 16 | 16 | 16 | 16 | 16 | 16 | 16 | 16 | 6 | 16 |
| | Temperature | °C | 45 | 45 | 45 | 45 | 45 | 45 | 45 | 45 | 25 | 25 | 35 |
| Operating condition (bottom) | Membrane | | GH | GH | GH | GH | GH | GE | GK | GK | GH | GK | GK |
| | TMP | bar | 16 | 16 | 16 | 16 | 16 | 16 | 16 | 16 | 12 | 10 | 4 |
| | Temperature | °C | 45 | 45 | 45 | 45 | 45 | 45 | 45 | 25 | 45 | 45 | 25 |

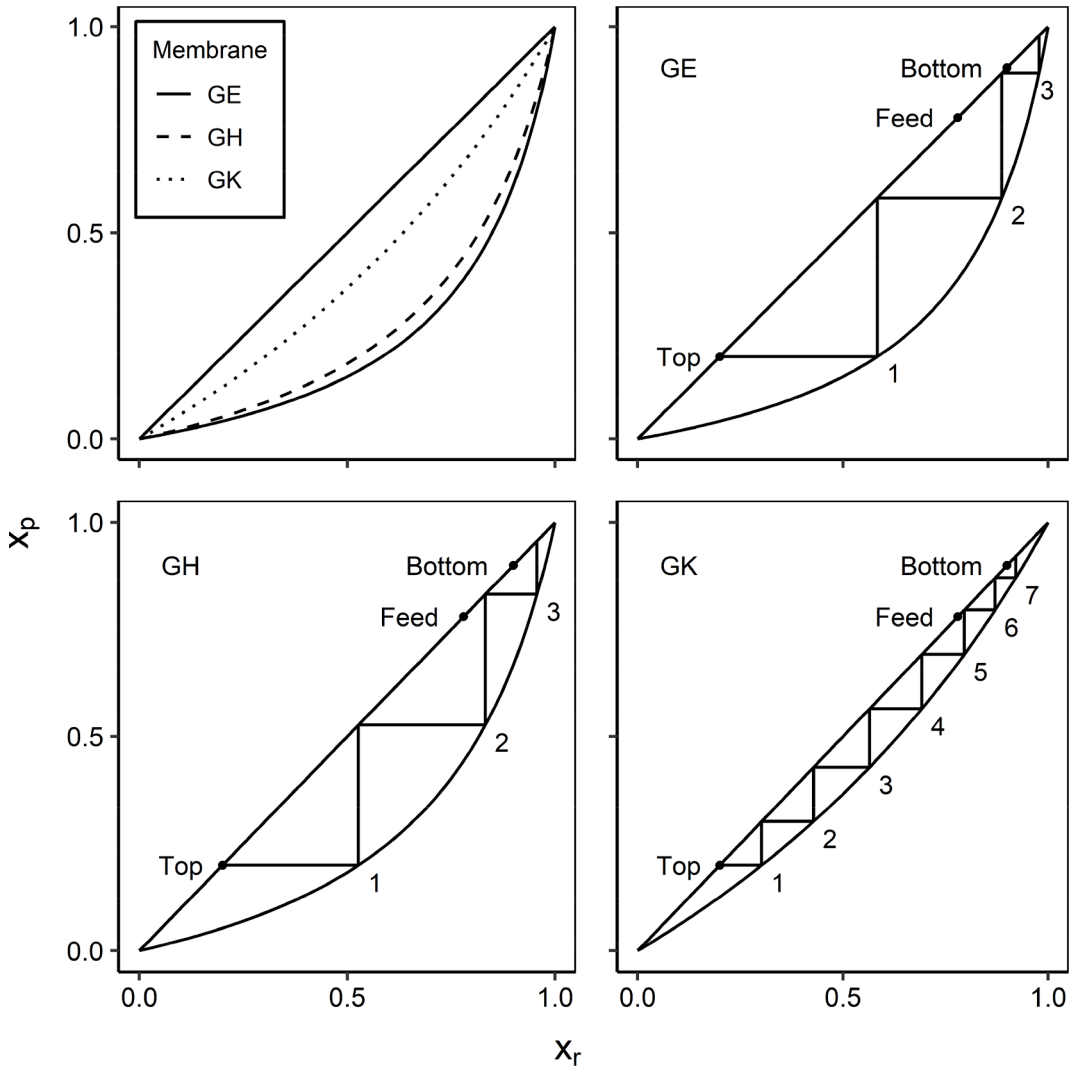


**Fig. 6.** Partitioning curve and minimum stage for GE, GH and GK membranes using TMP of 16 bar, temperature of 45 °C and stage cut of 0.6.

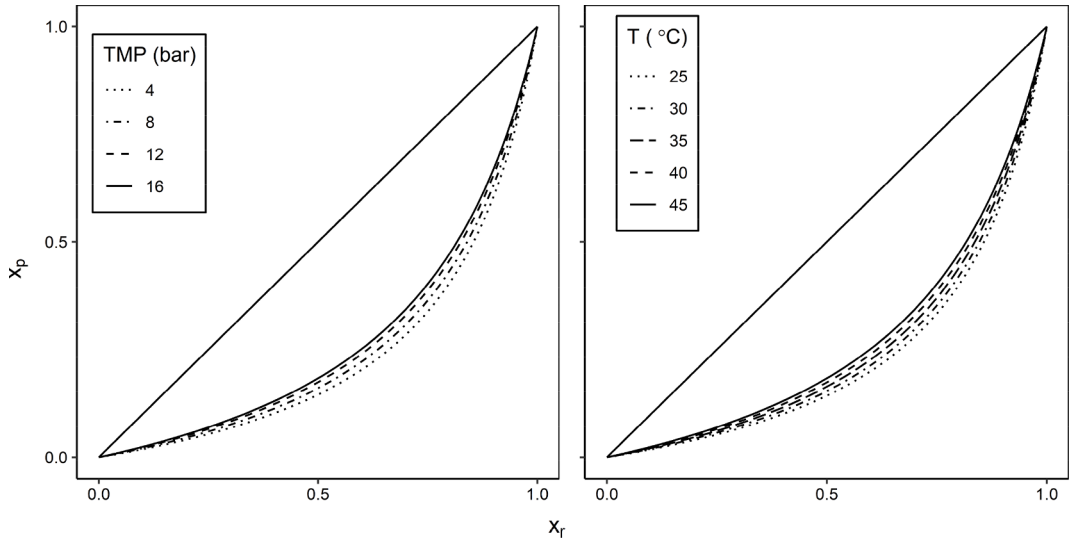


**Fig. 7.** Effect of TMP and operating temperature on the partitioning curve of GH membrane using a stage cut of 0.6.

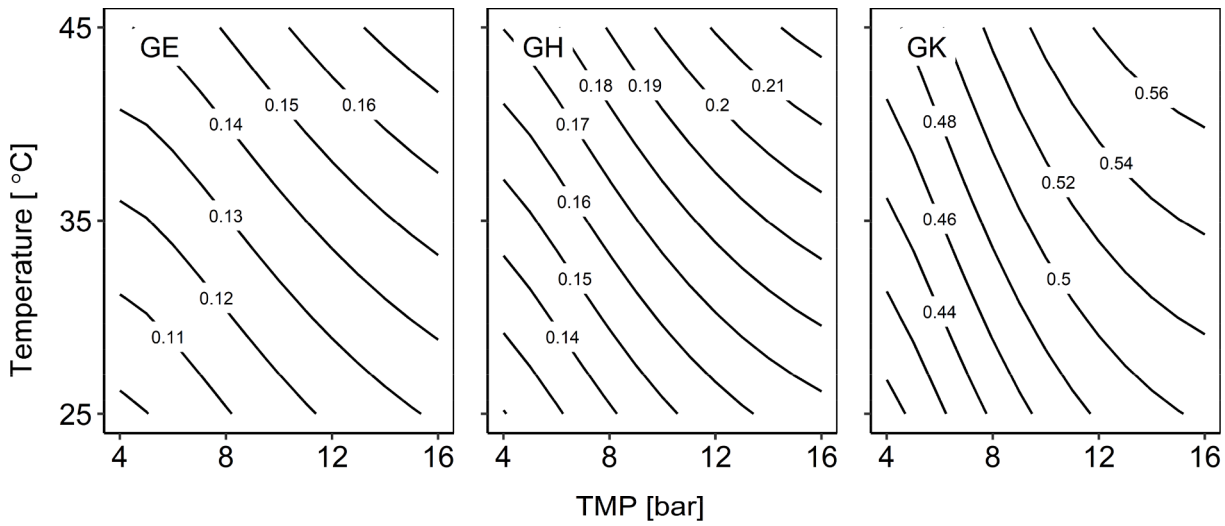


**Fig. 8.** Contour plot of the separation factor, $\alpha$, as a function of the TMP and the operating temperature for the 3 membranes.

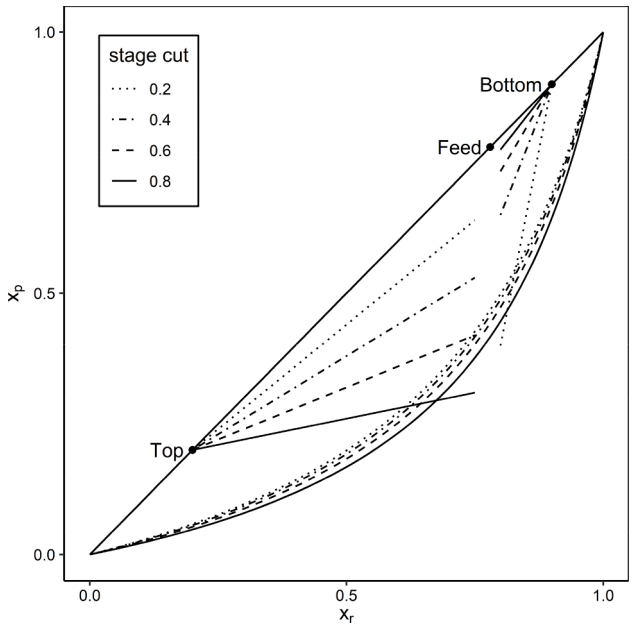


**Fig. 9.** Effect of the stage cut on the partitioning curve and the operating lines for the GH membrane using TMP of 16 bar and temperature of 45 °C (design A).

from the real rejection due to concentration polarization. However, we found that this is not a strong deviation. The flow conditions, defined by the stage cut, affected the partitioning curve only slightly.

The slopes of the operating lines become smaller at a larger stage cut. However, this works out differently for the 2 sections. For the top section, a lower slope means the operating line is situated further from the diagonal line. As a result, the number of stages required increases. On the other hand, a lower slope for bottom operating lines brings the line closer to the diagonal line and thus requires less stages in this section. To complete the design, the values of the stage cuts at both sections need to be selected such that both intersect as closely as possible to the feed composition. This implies that very high or low values of both stage cuts are not possible, because this would construct a design of both sections that would not meet each other.

As expressed in Eqs. (7)–(10), the slopes of the operating lines change at every stage. The slopes increase for the top operating lines and decrease for the bottom ones; thus, the lines for the subsequent stages are closer to the diagonal line. However, this does not change the fact that the value of the chosen stage cut affects the slope of the operating line (represented by the first stage); and it still necessitates the choice of a moderate stage cut value for both top and bottom sections.

We start from the top section downward, therefore we select the top stage cut at the start of the design. The stage cut at the bottom section will be adjusted to meet this selection. In view of the computational requirements, this method is better than adjusting both stage cuts at the same time. Here, we chose a top stage cut of 75% of its maximum. This value of 75% was chosen arbitrarily. The choice affects the number of stages and the membrane surface area required, and determines the stage cut for the bottom, which again influences the number of stages and the membrane surface area needed in that section.

Fig. 10 shows the effect of the stage cut on the required area for both sections. The stage cut at the top is $\theta_{top}$, and the bottom stage cut, $\theta_{bottom}$, is adjusted to meet this. The maximum value of $\theta_{top}$ was calculated by solving the operating line equation that crosses the partitioning curve with a retentate concentration similar to the feed. The minimum value was found computationally because no values below this minimum converged into a design with an adjusted $\theta_{bottom}$. For GH membranes with TMP of 16 bar and temperature of 45 °C, the maximum top stage cut was 0.716 and the minimum was 0.35.

Fig. 10a shows that the required area increased with increasing stage cut. This applied for both sections. This was as expected, because a larger stage cut implies a higher permeate flow and thus a larger area was needed, given a fixed flux at certain operating conditions. The difference between both sections was that the stage cut at the top could be chosen, whereas the bottom stage cut followed from the chosen stage cut at the top. The values of $\theta_{bottom}$ varied somewhat within the selected values of $\theta_{top}$, yet were all within a close range. Fig. 10c shows that the design had a short bottom section and a longer top section, because the concentration difference between the bottom target and the feed is far less than the difference between the top target and the feed.

As the design delivers a discrete value of the number of stages, it is logical that there are discontinuities in the required membrane surface area, and it also allows some freedom in the design resulting in the occasional selection of one more or less stage (e.g., at a stage cut of 0.4).

### 4.2. Design of the cascades

In this section, we demonstrate the design for the cascade using a uniform setup for the whole cascade. The membrane selection, the TMP and operating temperature were the same for each stage. The stage cut was constant for each section with a different value for top and bottom,

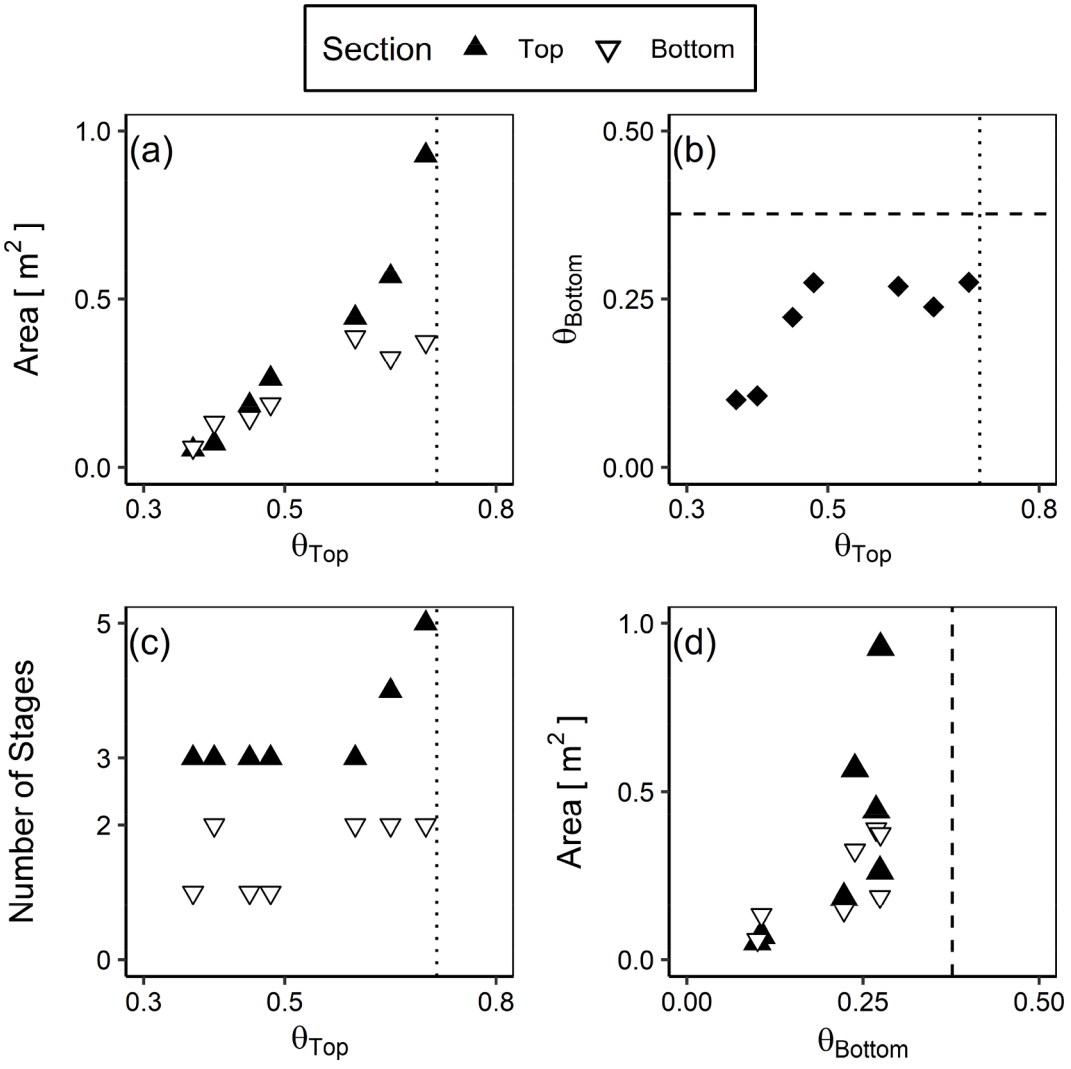


**Fig. 10.** Effect of the stage cut on the required area in both sections for the GH membrane operated with TMP of 16 bar and temperature of 45 °C (design A). The dotted line shows the maximum stage cut at the top section. The dashed line shows the maximum stage cut at the bottom section.

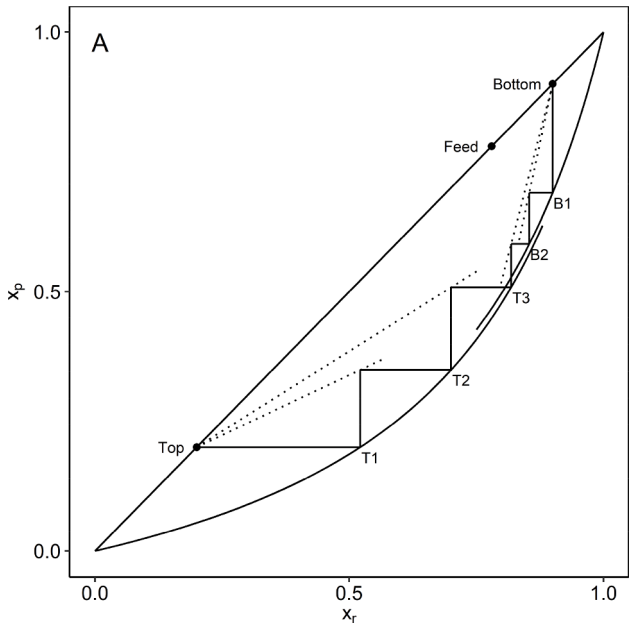


**Fig. 11.** McCabe-Thiele diagram of the 5-stage design of the fractionation cascade using GH membrane with TMP of 16 bar and temperature of 45 °C (design A). See Tables 2 and A.1 for further details.

so that the design meets at the feed.

Fig. 11 shows the McCabe-Thiele diagram for a 3 + 2 stage cascade for the reference design (A). The top stage cut maximum for this setup was found to be 0.71, therefore the design $\theta_{top}$ was set to 0.54. With this value, the stage cut for the bottom stage was found to be 0.22. Fig. 11 shows that this results in slightly different partitioning curves for the top and bottom sections (see Eqs. (5) and (6)).

The design consists of 3 stages in the top section and 2 stages in the bottom section, thus 5 stages in total. Therefore, we see 4 operating lines in the design that relate the compositions between adjacent stages. As a convention, we determine that the feed enters the last stage of the bottom section, represented here as stage B2. This stage was also operated with the stage cut of the bottom section, and thus connects with the bottom operating line.

Setting a different separation target requires recalculation and may result in a different design. Fig. 12 (top side) shows the designs of the cascade with top targets of 0.1 (B) and 0.3 (C). Compared with the reference (Fig. 11), design B was stretched toward the top section and required more stages. Design C had a similar number of required stages yet with a more compact design. From Figs. 12 and 11, we can also see that the bottom design for all 3 designs was different despite the similar bottom target. The stretch and compaction of the design can also be seen for designs D and E with different bottom targets. In this case, the design for the top section did not change.

Changing the top target to design B or C required a complete recalculation for both sections, whereas changing the bottom target to design D or E only affected the design at the bottom. The change in the top target affected the slope of the operating line that passed through the feed concentration at the partitioning curve and thus affected $\theta_{top,max}$. As a consequence, the operating $\theta_{top}$ also changed. Setting the stage cut constant was possible in principle; the choice of using 75% $\theta_{top,max}$ was arbitrary. However, the value must still be clearly lower than its maximum. In addition, a constant stage cut will still imply different slopes for different top targets, because the operating lines pivot on the target point (Eq. (12)). As a consequence, the design of the bottom section would also change despite having no change in the bottom target. In the other case, changing the bottom target would only affect the design at the bottom because there is no change at the top section.

A similar design procedure could be applied with other membranes resulting in a 3 + 2 stage design with GE membranes and a 7 + 2 stage design with GK membranes (Fig. A.1). The designs follow our expectations considering the shape of their partitioning curves (Fig. 6).

The required membrane area per stage for GH, GE and GK cascades (designs A, F and G) is shown in Fig. 13. The required areas for GH and GE are in the same range, whereas the required area for the GK membrane cascade is much higher. Both GE and GH membrane cascades require the same number of stages at both sections. The GE membrane has a lower flux and as a result, the area requirement was slightly higher compared with the GH membrane cascade (Fig. 13). The GK membrane has a higher flux than the other 2 membranes, which would suggest the requirement of less area. In fact, the design with the GK membranes required significantly more membrane area than the other 2 membranes. The reason for this is the large number of stages. The whole section was operated with a fixed stage cut, therefore, it is logical that the membrane near the feed processes a larger flow rate, and thus requires a larger area. The more stages that are required in a section, the more this flow accumulates, resulting in a much larger required area. Fig. 13 illustrates the area distribution among stages in the cascades. This result also supports a previous study on the inhomogeneous cascades, which reported a larger area requirement at the feed stage [18].

### 4.3. Hybrid design of the cascades

The design procedure suggests that we use different values for the stage cut for both sections such that the design meets at the feed. As a consequence, the partitioning curves for the 2 sections are not the same. However, the difference was small due to the small effect of the stage cut on the partitioning curve (Section 4.1.2). Nevertheless, this does show that working with different partitioning curves for both sections is possible. In this case, one can also achieve that by using different membranes. This will indeed result in a larger difference in the partitioning curves for top and bottom. Apart from the choice of membrane and the stage cut, the operating TMP and temperature affect the partitioning curve and may be used to tune the curve.

In Fig. 14, we demonstrate 4 hybrid designs (designs H–K) using arbitrarily chosen combinations of setup conditions at the top and bottom sections. All designs were constructed to reach a $x_{p,top}$ of 0.2 and a $x_{r,bottom}$ of 0.9. Constant conditions (membrane, TMP, temperature and stage cut) were applied for all stages within a particular section. The selection of the design variables for these designs is shown in Table 2. The details of these designs are provided in Table A.1.

Unlike the previous studies on membrane cascades, the target in the design using the McCabe-Thiele method is not achieving a certain purity, because this is a constraint imposed on all designs. The design procedure in fact helps to minimize the number of stages, the membrane area requirement, and to maximize the yield of a specific product (either top or bottom). Using a hybrid design may help achieve these targets, because the stage requirement at the bottom was not really affected by the choice of membranes and the top design is more compact using GE or GH membranes. On the other hand, using GK membranes at a similar number of stages may reduce the surface area requirement, because this membrane features a larger flux. However, a lower number of stages does not guarantee a lower total membrane surface area requirement.

The total area requirement is closely related to the overall system cut. This parameter is dependent on the stage cut at both sections (Eqs. (15)–(19)). We can see a clear relationship between the stage cut at the top with the membrane, the TMP and the temperature. However, the relationship of those operating conditions with the bottom stage cut was unclear, because it was determined iteratively such that the operating lines crossed at composition of the feed. One critical issue that was found during the design is that the chance of finding a converged iteration (in order to find the bottom stage cut) was less when the difference between 2 partitioning curves was large. This was the case, for example, with design J (Fig. 14), which had small separation steps at the bottom

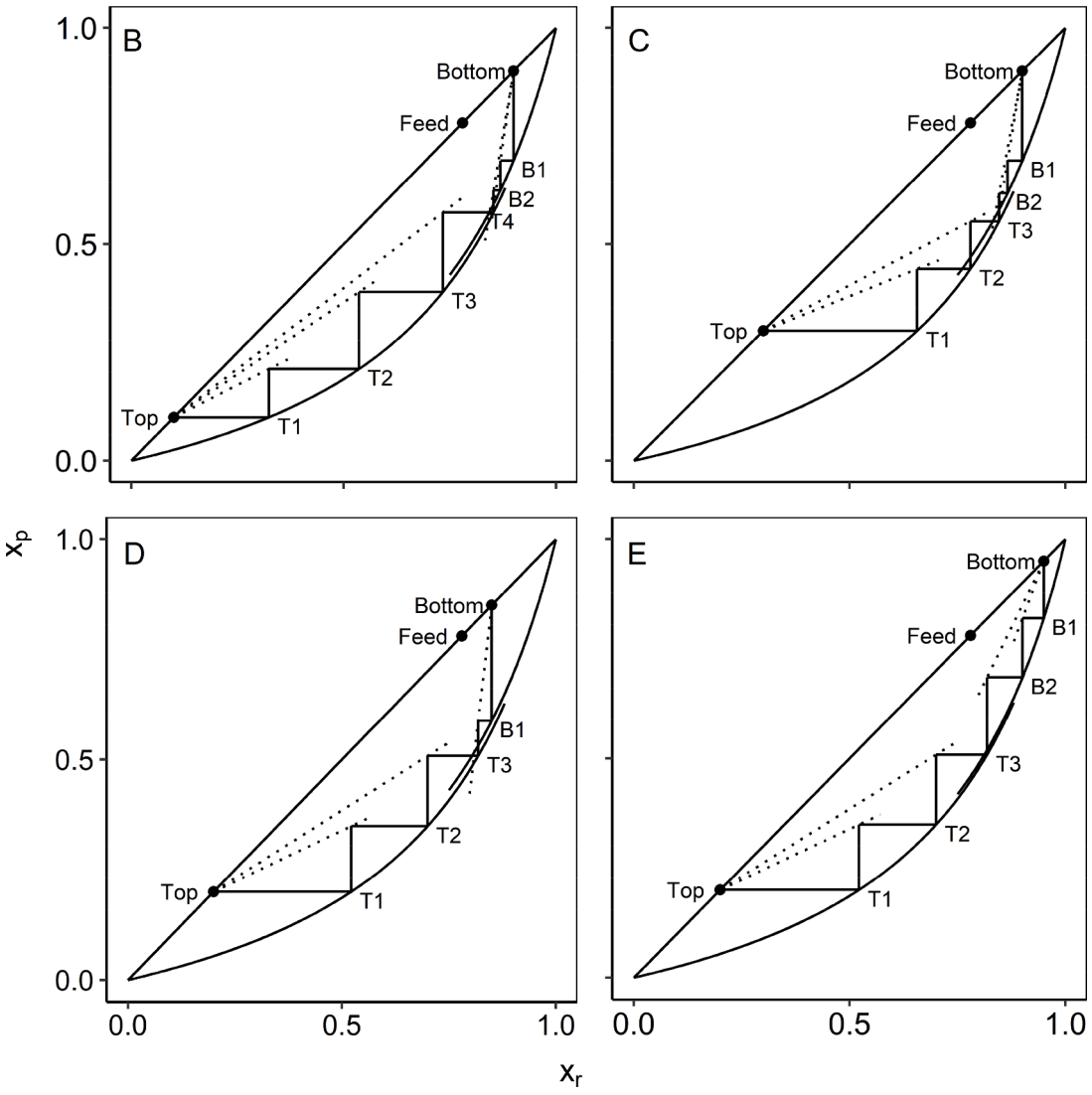


**Fig. 12.** McCabe-Thiele diagram of the membrane cascade design with various targets using the GH membrane operated with TMP of 16 bar and temperature of 45 °C. Top side shows a top target, $x_{p,\text{top}}$, of 0.1 (design B) and 0.3 (design C) with a bottom target, $x_{r,\text{bottom}}$, of 0.9. The bottom side shows a bottom target, $x_{r,\text{bottom}}$, of 0.85 (design D) and 0.95 (design E) with a top target, $x_{p,\text{top}}$, of 0.2.

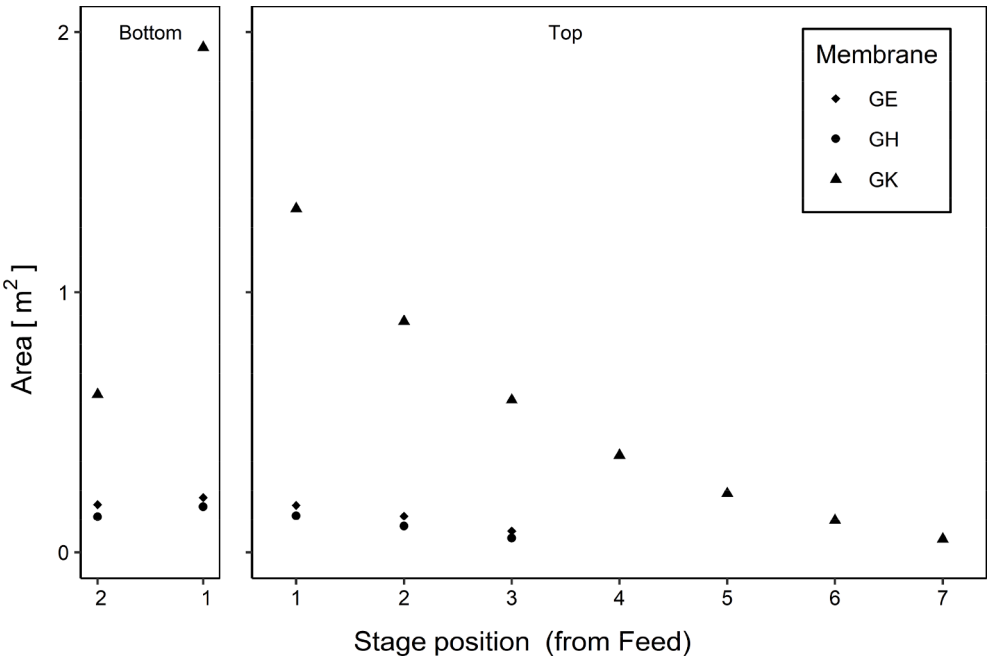


**Fig. 13.** Area distribution among the stages in the design of membrane cascades using GE, GH and GK membranes operated at 16 bar and 45 °C (designs F, A and G).

section. The exact values of maximum difference between partitioning curves cannot be established using the current method. However, as a general guideline we can reduce the difference in the partitioning curves by selecting separation factors, $\alpha$, that are close between each other. The contour plots in Fig. 8 can be useful in selecting the separation factors.

The ability of using a different set up for different sections indicates further possibility of using independent set up within sections. This concept will allow the usage of different membrane, TMP and temperature for every stage. Moreover, each stage can be operated using different stage cut. This complex design is also supported by the nature of the McCabe-Thiele approach for membrane cascades that requires an evaluation of operating lines for every stage. At the same time, finding the minimum amount of membrane surface area may require balancing all the different parameters, for which a numerical procedure would probably be preferred. Therefore, further development is needed to make the method more robust for numerical evaluation.

In our work, the stage cut was defined based on mass flow (equation (4)). The stage cut can also be defined by considering the molar ratio of the solutes in the permeate and the feed. This definition requires a correction of equation (4). This corrected stage cut is then used in the operating lines (equation (7)–(12)). Using this corrected stage cut will limit the possibility of the stage cut value that is usable for the design. This issue occurred due to the fact that both stage cuts are by definition fractions that have maximum values of 1. Nevertheless, considering this correction in the future research can improve the robustness of this design method. However, this also challenge a development of a numerical optimization method to find the suitable stage cut value that gives a converged design and an optimum performance.

## 5. Conclusions

We developed a method to design an inhomogeneous membrane cascade to purify a FOS mixture by adapting the classic McCabe-Thiele approach for distillation. The method determines the number of stages needed and the required membrane surface area in the cascade to achieve specific target compositions for both products: small mono- and disaccharides and larger oligosaccharides. As an independent design parameter, the stage cut should be defined before the design procedure.

The procedure starts from the top section followed by the bottom section. The membrane selection, TMP, temperature and stage cut in any stage within 1 section are uniform. Nevertheless, the method allows us to use different combinations of membranes and operating conditions in both sections (hybrid design).

Apart from the selection of the membranes, TMP and temperature, the stage cut value strongly determines the required number of stages and the total membrane surface area of the cascades. The lower the overall stage cut, the larger the internal recycle is and the larger the membrane surface area is for a given feed volume. However, the overall system cut depends on the stage cuts of the top and bottom sections, which were determined separately. The value of the bottom stage cut was calculated iteratively to match its design with the that of the top section. However, the relationship between both stage cuts is not trivial and is now found iteratively. To obtain an optimal design using possible combinations of the available membrane, TMP and temperature, further adaptation toward a robust numerical optimization procedure is important.

## CRediT authorship contribution statement

**Zulhaj Rizki:** Conceptualization, Methodology, Software, Formal analysis, Investigation, Writing - original draft, Writing - review & editing, Visualization. **Anja E.M. Janssen:** Conceptualization, Writing - review & editing, Supervision. **Albert van der Padt:** Conceptualization, Writing - review & editing, Supervision. **Remko M. Boom:** Conceptualization, Writing - review & editing, Supervision.

## Declaration of Competing Interest

The authors declare that they have no known competing financial interests or personal relationships that could have appeared to influence the work reported in this paper.

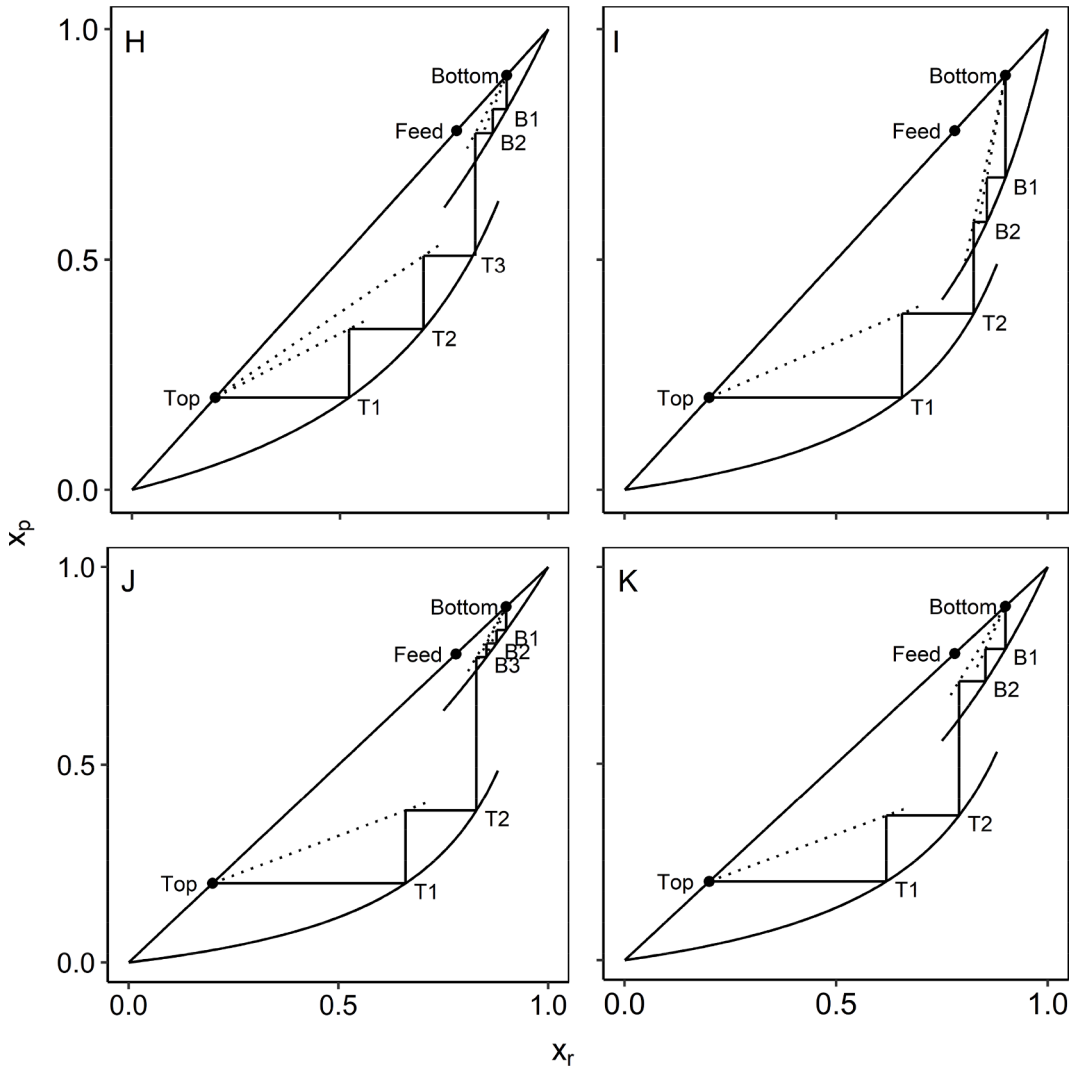


**Fig. 14.** McCabe-Thiele diagram for selected hybrid membrane cascade designs. For the design decisions, refer to Table 2.

## Acknowledgements

The authors would like to acknowledge Lembaga Pengelola Dana Pendidikan (LPDP) and Kementrian Keuangan Indonesia for financial support.

## Appendix A. Supplementary material

Supplementary data to this article can be found online at https://doi.org/10.1016/j.seppur.2020.118094.

## References

[1] A. Franck, Technological functionality of inulin and oligofructose., Br. J. Nutr. 87 Suppl 2 (2002) S287–S291. https://doi.org/10.1079/BJNBJN/2002550.
[2] G. Flamm, W. Glinsmann, D. Kritchevsky, L. Prosky, M. Roberfroid, Inulin and oligofructose as dietary fiber: a review of the evidence, Crit. Rev. Food Sci. Nutr. 41 (2001) 353–362, https://doi.org/10.1080/20014091091841.
[3] A. Tárrega, J.D. Torres, E. Costell, Influence of the chain-length distribution of inulin on the rheology and microstructure of prebiotic dairy desserts, J. Food Eng. 104 (2011) 356–363, https://doi.org/10.1016/j.jfoodeng.2010.12.028.
[4] J.R. Hess, A.M. Birkett, W. Thomas, J.L. Slavin, Effects of short-chain fructooligosaccharides on satiety responses in healthy men and women, Appetite 56 (2011) 128–134, https://doi.org/10.1016/j.appet.2010.12.005.
[5] W. Li, J. Li, T. Chen, C. Chen, Study on nanofiltration for purifying fructo-oligosaccharides I. Operation modes, J. Memb. Sci. 245 (2004) 123–129, https://doi.org/10.1016/j.memsci.2004.07.021.
[6] A.K. Goulas, P.G. Kapasakalidis, H.R. Sinclair, R.A. Rastall, A.S. Grandison, Purification of oligosaccharides by nanofiltration, J. Memb. Sci. 209 (2002) 321–335, https://doi.org/10.1016/S0376-7388(02)00362-9.
[7] R.C. Kuhn, F. Maugeri Filho, V. Silva, L. Palacio, A. Hernández, P. Prádanos, Mass transfer and transport during purification of fructooligosaccharides by nanofiltration, J. Memb. Sci. 365 (2010) 356–365, https://doi.org/10.1016/j.memsci.2010.09.031.
[8] T.M.K.C. Khulbe, C. Feng, The art of surface modification of synthetic polymeric membranes, Polym. Polym. Compos. 21 (2013) 449–456, https://doi.org/10.1002/app.
[9] B.S. Lalia, V. Kochkodan, R. Hashaikeh, N. Hilal, A review on membrane fabrication: structure, properties and performance relationship, Desalination 326 (2013) 77–95, https://doi.org/10.1016/j.desal.2013.06.016.
[10] A. Caus, L. Braeken, K. Boussu, B. Van der Bruggen, The use of integrated countercurrent nanofiltration cascades for advanced separations, J. Chem. Technol. Biotechnol. 84 (2009) 391–398, https://doi.org/10.1002/jctb.2052.
[11] A. Córdova, C. Astudillo, L. Santibañez, A. Cassano, R. Ruby-Figueroa, A. Illanes, Purification of galacto-oligosaccharides (GOS) by three-stage serial nanofiltration units under critical transmembrane pressure conditions, Chem. Eng. Res. Des. 117 (2017) 488–499, https://doi.org/10.1016/j.cherd.2016.11.006.
[12] N.V. Patil, T. Schotel, C.V. Rodriguez Gomez, V. Aguirre Montesdeoca, J.J. W. Sewalt, A.E.M. Janssen, R.M. Boom, Continuous purification of galacto-oligosaccharide mixtures by using cascaded membrane filtration, J. Chem. Technol. Biotechnol. 91 (2016) 1478–1484, https://doi.org/10.1002/jctb.4746.
[13] J.C. Te Lin, A.G. Livingston, Nanofiltration membrane cascade for continuous solvent exchange, Chem. Eng. Sci. 62 (2007) 2728–2736, https://doi.org/10.1016/j.ces.2006.08.004.
[14] W.E. Siew, A.G. Livingston, C. Ates, A. Merschaert, Continuous solute fractionation with membrane cascades – a high productivity alternative to diafiltration, Sep. Purif. Technol. 102 (2013) 1–14, https://doi.org/10.1016/j.seppur.2012.09.017.
[15] R.S. Herbst, F.P. McCandless, No-mix and ideal separation cascades, Sep. Sci. Technol. 29 (1994) 2215–2226, https://doi.org/10.1080/01496399408003175.

[16] E.N. Lightfoot, T.W. Root, J.L. O'Dell, Emergence of ideal membrane cascades for downstream processing, Biotechnol. Prog. 24 (2008) 599–605, https://doi.org/10.1021/bp070335l.
[17] N.V. Patil, X. Feng, J.J.W. Sewalt, R.M. Boom, A.E.M. Janssen, Separation of an inulin mixture using cascaded nanofiltration, Sep. Purif. Technol. 146 (2015) 261–267, https://doi.org/10.1016/j.seppur.2015.03.061.
[18] V. Aguirre Montesdeoca, A. Van der Padt, R.M. Boom, A.E.M. Janssen, Modelling of membrane cascades for the purification of oligosaccharides, J. Memb. Sci. 520 (2016) 712–722, https://doi.org/10.1016/j.memsci.2016.08.031.
[19] Z. Rizki, A.E.M. Janssen, R.M. Boom, A. van der Padt, Oligosaccharides fractionation cascades with 3 outlet streams, Sep. Purif. Technol. 221 (2019) 183–194, https://doi.org/10.1016/J.SEPPUR.2019.03.086.
[20] Z. Rizki, A.E.M. Janssen, G.D.H. Claassen, R.M. Boom, A. van der Padt, Multi-criteria design of membrane cascades: selection of configurations and process parameters, Sep. Purif. Technol. (2019), https://doi.org/10.1016/j.seppur.2019.116349.
[21] Z. Rizki, A.E.M. Janssen, E.M.T. Hendrix, A. van der Padt, R.M. Boom, G.D.H. Claassen, Design optimization of a 3-stage membrane cascade for oligosaccharides purification using a mixed integer non-linear programming, 2020. Manuscript submitted for publication.
[22] W.L. McCabe, E.W. Thiele, Graphical Design of Fractionating Columns, 1925. https://doi.org/10.1021/ie50186a023.
[23] F.P. McCandless, A comparison of membrane cascades, some one-compressor recycle permeators, and distillation, J. Memb. Sci. 89 (1994) 51–72, https://doi.org/10.1016/0376-7388(93)E0208-2.
[24] A. Lejeune, M. Rabiller-Baudry, T. Renouard, Design of membrane cascades according to the method of McCabe-Thiele: an organic solvent nanofiltration case study for olefin hydroformylation in toluene, Sep. Purif. Technol. 195 (2018) 339–357, https://doi.org/10.1016/j.seppur.2017.12.031.
[25] F.P. McCandless, A comparison of countercurrent recycle membrane cascades with some "One-Compressor" recycle permeators for gas separations in terms of ideal crossflow stages, Sep. Sci. Technol. 31 (1996) 729–756, https://doi.org/10.1080/01496399608001321.
[26] W.E. Siew, A.G. Livingston, C. Ates, A. Merschaert, Molecular separation with an organic solvent nanofiltration cascade – augmenting membrane selectivity with process engineering, Chem. Eng. Sci. 90 (2013) 299–310, https://doi.org/10.1016/j.ces.2012.10.028.
[27] J. Vanneste, S. De Ron, S. Vandecruys, S.A. Soare, S. Darvishmanesh, B. Van Der Bruggen, Techno-economic evaluation of membrane cascades relative to simulated moving bed chromatography for the purification of mono- and oligosaccharides, Sep. Purif. Technol. 80 (2011) 600–609, https://doi.org/10.1016/j.seppur.2011.06.016.
[28] T. Renouard, A. Lejeune, M. Rabiller-Baudry, Separation of solutes with an organic solvent nanofiltration cascade: designs, simulations and systematic study of all configurations, Sep. Purif. Technol. 194 (2018) 111–122, https://doi.org/10.1016/j.seppur.2017.11.029.
[29] Z. Rizki, E. Suryawirawan, A.E.M. Janssen, A. van der Padt, R.M. Boom, Modelling temperature effects in a membrane cascade system for oligosaccharides, J. Memb. Sci. (2020), 118292, https://doi.org/10.1016/j.memsci.2020.118292.
[30] M.S. Avgidou, S.P. Kaldis, G.P. Sakellaropoulos, Membrane cascade schemes for the separation of LPG olefins and paraffins, J. Memb. Sci. 233 (2004) 21–37, https://doi.org/10.1016/j.memsci.2003.12.007.
[31] S.-T. Hwang, K. Kammermeyer, Operating lines in cascade separation of binary mixtures, Can. J. Chem. Eng. 43 (1965) 72, https://doi.org/10.1002/cjce.5450430205.
[32] V. Aguirre Montesdeoca, J. Bakker, R.M. Boom, A.E.M. Janssen, A. Van der Padt, Ultrafiltration of non-spherical molecules, J. Memb. Sci. 570–571 (2019) 322–332, https://doi.org/10.1016/j.memsci.2018.10.053.